JOURNAL OF CATALYSIS 58, 396–408 (1979)

Effect of Cobalt Ion Dispersion on H_2–D_2 Equilibration and Other Simple Reactions Catalyzed by CoO–MgO Solid Solutions

V. INDOVINA, A. CIMINO, M. INVERSI, AND F. PEPE

Centro di studio del CNR su "Struttura e attività catalitica di sistemi di ossidi," Istituto di Chimica Generale ed Inorganica dell'Università di Roma, Roma, Italy

Received June 6, 1978

Solid solutions of CoO–MgO, with Co/Mg ratios from 1 to 50, have been studied as catalysts for the H_2–D_2 equilibration reaction. This paper presents data in the temperature range above 300 K (high temperature range, HTR). The catalytic activity per cobalt ion increases with cobalt content. A statistical analysis of the surface configurations shows that the turnover number (molecules per second per site) is a constant if the active site is a cluster containing at least a pair of cobalt ions. The mechanism of the HTR reaction is then discussed. Comparison of the concentration dependence for the N_2O decomposition reaction, and for the CO oxidation, shows that the former shows a decrease of activity per site with increasing Co^{2+} content ("dilution effect"), which cannot be explained on the basis of configuration requirements only, while the second reaction shows a constant turnover number, implying a configuration-insensitive reaction. The data suggest details on the mechanisms.

INTRODUCTION

The study of catalysts made by dispersing active transition metal ions (*tmi*) in an inert matrix has been pursued in our laboratory as well as in others (*1–3*) in view of the potential offered by this type of system to study the (i) influence of the electronic configuration of the *tmi*; (ii) role of the *tmi–tmi* interactions; (iii) influence of the symmetry of the site occupied by the *tmi*; and (iv) effect of the matrix environment on catalytic activity.

Results obtained for the N_2O decomposition on *tmi* dispersed in MgO typically show a decrease of the activity per ion with increasing concentration of *tmi*, the so-called "dilution effect," which can be expressed by the variation of the absolute rate constant k_{abs} referred to unit concentration, k_{abs}/x, where x is the mole fraction of *tmi*. The same effect can be expressed by the variation of the *turnover number* (molecules reacted per site and per second) with the *tmi* concentration. The CoO–MgO system is a good example, since Co^{2+} ions are very active for the decomposition reaction and a wide range of x values has accordingly been studied (*4*).

The fact that the activity per ion is not constant can be seen within the classification originally proposed by Boudart for metals (*5*), thus the N_2O reaction on oxides is classified as *structure-sensitive*. The cause of the structure-sensitivity, however, is not necessarily the requirement for a particular geometric arrangement of atoms in the active site. In fact, a structure-sensitivity arises if a step controlling the molecular mechanism involves the breaking or the formation of a bond whose strength depends on the active-ion concentration.

0021-9517/79/090396-13$02.00/0

In the example quoted, N_2O decomposition, the steps involved are thought to be the oxygen adsorption–desorption processes. Furthermore, since the (*tmi*)/(matrix ions) concentration ratio varies with the *tmi* concentration, a contribution to the dilution effect may arise from a participation of the matrix ions in one of the steps.

In the case of *tmi* dispersions in oxide matrices, the structure-sensitivity may also be directly linked to the mechanism of the reaction, as in the case of metals. It is therefore of interest to investigate simple reactions taking place on the same oxide system, and to look for their classification, in order to obtain insight into the nature of the active site and of the reaction mechamism. Within this framework, we have studied the H_2–D_2 equilibration reaction in CoO–MgO solid solutions. This paper also compares the *tmi* concentration dependence of the catalytic activity for the three reactions: H_2–D_2 equilibration, N_2O decomposition (*4*), and CO oxidation (*6*), which have been carried out on the same catalytic system; the details and results of the last two reactions were reported in the original papers.

EXPERIMENTAL

Catalysts. CoO–MgO solid solutions used in the present work are from the same batch as those reported in Ref. (*4*), where details of the preparation, chemical analysis, and structural and magnetic properties are given. Note that the CoO–MgO system forms a continuous range of solid solutions and that the specimens used in the present work were shown to be true solid solutions (*7*).

Although no direct inspection of the surface composition has yet been made, the study of the analogous system NiO–MgO by photoelectron spectroscopy has not revealed marked changes of composition at the surface in comparison to the bulk (*8*). The surface composition can therefore be taken as approximated by the bulk composition.

Samples are designated as MCo, followed by a figure which gives the nominal cobalt content expressed as Co atoms per 100 Mg atoms. Surface areas values (square meters per gram), determined by Kr adsorption at 77 K, are indicated in parentheses after each catalyst: MgO (19), MCo 1 (14), MCo 10 (4.3), MCo 20 (0.6), MCo 50 (0.5), CoO (0.2).

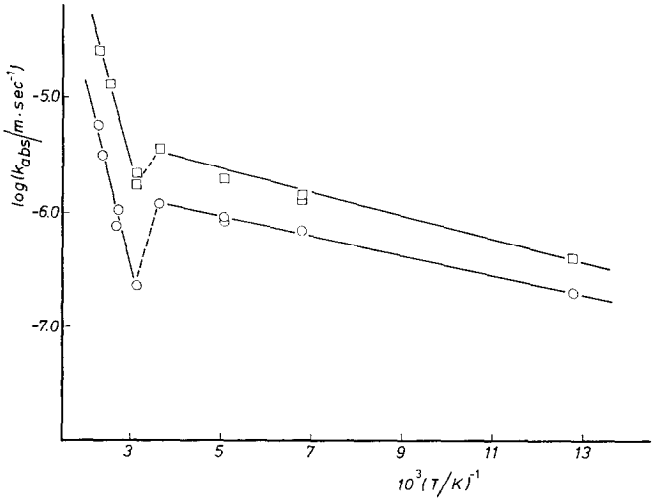

FIG. 1. A plot of $\log(k_{abs}$ per meter per second) vs 10^3 $(T/K)^{-1}$ for the H_2–D_2 equilibration on MCo 20 (○) and on MCo 50 (□) catalysts.

Catalytic experiments. H_2–D_2 equilibration experiments were carried out in the circulating system described previously (*9*). An approximately equimolar mixture of H_2–D_2 at about 40 Torr was circulated through a silica reactor containing the catalyst (0.1–0.3 g) previously activated *in vacuo* at 800 K. Between experiments, samples were evacuated for 30 min at 800 K. A sample of 3 ml of gas was withdrawn at regular intervals (generally 3 min) and was brought to a Nier-type mass spectrometer for analysis. Kinetic constants for the H_2–D_2 equilibration were calculated as absolute first-order rate constants (k_{abs} per meter per second) as previously reported (*9*). Hydrogen was purified by passing it through a Pd thimble (*9*).

RESULTS

The catalytic activity for the equilibration reaction was investigated in the temperature range 78 to 500 K for the solid solution specimens reported above. The Arrhenius plot over the whole temperature range shows a discontinuity, as exemplified by MCo 20 and by MCo 50 in Fig. 1, which divides the entire range into two regions, one above about 300 K (hereafter called the high temperature region, HTR) and one below (the low temperature region or LTR). The work reported and discussed here refers to the HTR, and Fig. 2 reports the Arrhenius plots for this temperature range, for the whole series of catalysts.

The distinction between the two regions is apparent not only via the marked difference in the apparent activation energies E_a, as seen from Fig. 1, but also in the kinetic behavior. The k_{abs} values in the HTR tend to decrease as the reaction proceeds and accordingly only initial values have been considered. By way of contrast, in the LTR the k_{abs} values were independent of time. The E_a values in the HTR were constant, and equal to about 29.3 kJ mol^{-1}; in the LTR they were about 4.2 kJ mol^{-1}.

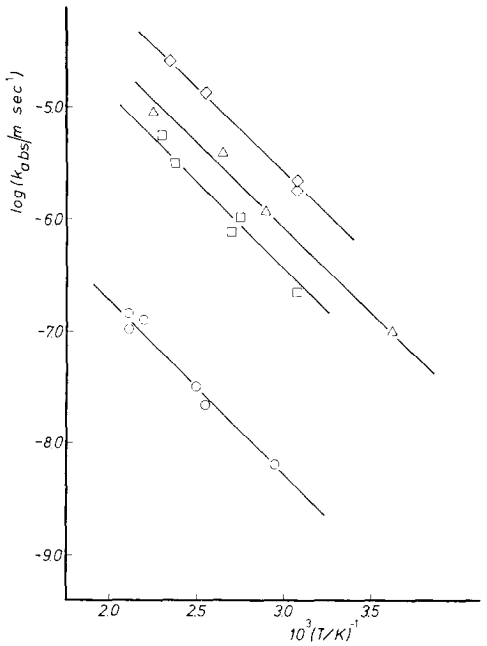

FIG. 2. H_2–D_2 equilibration. A plot of log(k_{abs} per meter per second) vs 10^3 $(T/K)^{-1}$. ○, MCo 1; △, MCo 10; □, MCo 20; ◇, MCo 50.

The existence of distinct ranges for the H_2–D_2 reaction has been proven for other systems, namely, CrO_x–SiO_2 (*10*), CrO_x–MgO (*9*), Cr_2O_3–Al_2O_3 (*11*), and $MgAl_{2-x}Cr_xO_4$ (*12*). While the boundary between the two temperature regions may depend on the catalyst, and hence a defined temperature cannot be given, the behavior indicates that different mechanisms may operate (*9*, *10*). This conclusion is based on experimental evidence from adsorption–desorption experiments, infrared spectroscopy, and catalysis results on various oxides (*13–15*).

DISCUSSION

1. *Turnover Numbers for H_2–D_2 Equilibration and Cobalt Concentrations*

The catalytic activity of CoO–MgO solid solutions for H_2–D_2 equilibration markedly increases with increasing cobalt content. N_2O decomposition (*4*) and CO oxidation (*6*) are also catalyzed by the same oxide

solid solutions, and show an activity dependent on the cobalt content. In the following discussion it will be shown that inspection of the dependence of catalytic activity on cobalt concentration can give valuable information on the nature of the active sites involved in each reaction. In this way the solid solution approach provides a means of investigating reaction mechanisms.

In fact, for a given reaction taking place on a series of catalysts, differences in specific velocities R (molecules per square meter per second) can arise from the variation of the activation energy and/or of the pre-exponential factor. However, in the case of both CO oxidation and of H_2–D_2 equilibration, the data show that the energy parameter remains fairly constant in each case. It is rather unlikely that the constancy of E_a for each type of reaction can be attributed to a simultaneous variation of the true activation energy and of the heats of adsorption of the kinetically significant species (*16*). Thus the differences in rates can be atrributed to the variation of the pre-exponential factor only. On the other hand, the entropic part of the pre-exponential factor referring to the molecular active complex is expected to be constant when the same reaction is investigated on the solid solutions of the same ion in the same matrix if, as the constancy of E_a suggests, the same mechanism operates. It then appears reasonable to conclude that the differences in rates are due only to the variation of active site concentrations. Under these circumstances, true turnover numbers N, i.e., R values normalized per active site concentration, are expected to be independent of cobalt content. However, since neither the concentration nor the nature of the active sites is known *a priori*, some assumptions must be made (and subsequently tested). Thus, an average turnover number per ion ($N_{ion} = R/[Co^{2+}]_{surf.}$) can be calculated by assuming: (i) that all Co^{2+} ions on the surface are potential sites and (ii) that the Co^{2+} surface concentration ($[Co^{2+}]_{surf.}$) is equal to the bulk concentration, as mentioned above. When this is done the plot of Fig. 3 is obtained, in which the N_{ion} values, calculated at two temperatures (455 and 555 K), are reported for the H_2–D_2 equilibration. The same figure also shows the dependence of N_{ion} for the other two reactions considered here, CO oxidation and N_2O decomposition.

Three distinct patterns emerge with regard to N_{ion}: (i) This parameter is roughly constant for the oxidation of CO; (ii) it strongly decreases with cobalt concentration for the decomposition of N_2O; and (iii) it increases (although in a non-uniform manner) with cobalt concentration for the equilibration reaction.

It should be stressed that the dependence of N_{ion} on the cobalt concentration is substantially the same at different temperatures, although some details change. Thus, in the case of CO oxidation, N_{ion} is roughly constant for all specimens at 455 K, while at 555 K the most dilute specimen, MCo 0.1, displays an N_{ion} value from four to eight times larger than the more concentrated specimens. However, the E_a value for MCo 0.1 and the activity level (both close to those of pure MgO) show that at high temperature, sites different from those operating at 455 K may predominate, thus rendering the comparison of MCo 0.1 with the other solid solution specimens less significant. In the case of N_2O decomposition, the variation of N_{ion} is larger at high temperature because the E_a values depend on cobalt concentration, but the drop is still very marked even at 455 K. Finally, the complex behavior of the equilibration reaction renders a detailed analysis more difficult, but it emerges that even if the activity per ion is considered, the more concentrated specimens are substantially more active (20 times) than the dilute one.

Active surface configurations. The con-

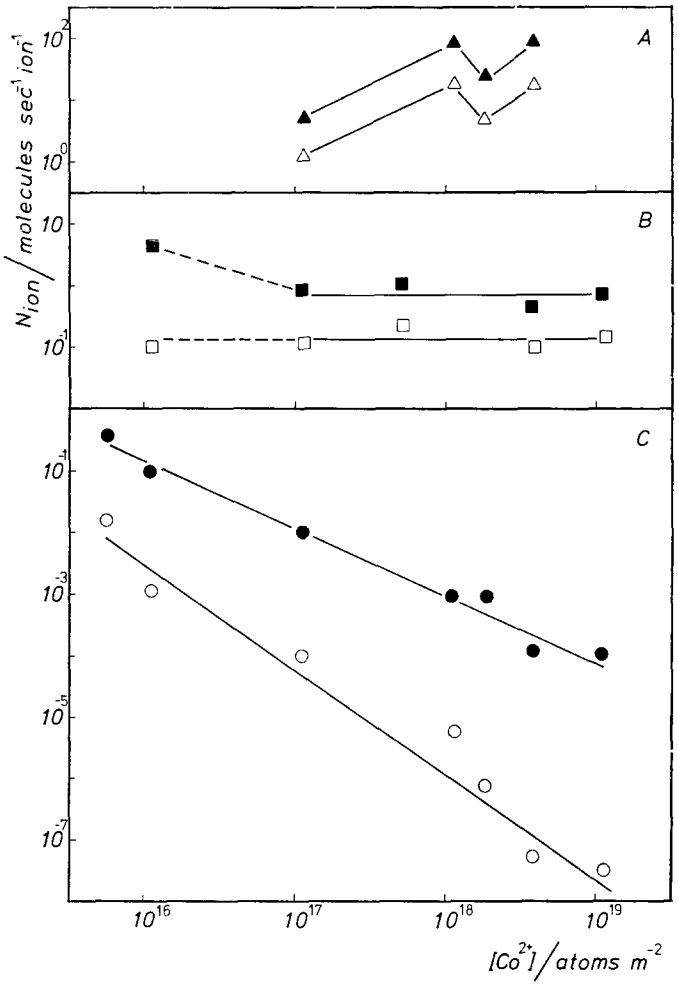

FIG. 3. Turnover numbers per cobalt ion (N_{ion} per molecules per second per ion) vs surface cobalt concentration (Co per atoms per square meter), for H_2–D_2 (*A*) for CO + O_2 (*B*), and for N_2O decomposition (*C*). H_2–D_2: △, 455 K; ▲, 555 K. Co + O_2: □, 455 K; ■, 555 K. N_2O: ○, 455 K; ●, 555 K.

stancy of N_{ion} for CO oxidation (Fig. 3) strongly suggests that all surface Co^{2+} ions (or a *constant fraction* of them) are the active sites for CO. By way of contrast, the variation of N_{ion} for H_2–D_2 equilibration shows that the fraction of the cobalt ions involved cannot be constant as their concentration is varied. Thus, (i) the active sites represent only a fraction of the surface cobalt present, and (ii) this fraction changes drastically with the cobalt content.

If we now focus attention on the catalyst, and investigate a property which can account for the variation of N_{ion}, it is clear that several of the properties of the solid vary, when the cobalt content is increased, in a way not proportional to the cobalt content. The concentration of a particular ionic configuration (e.g., isolated Co^{2+}, Co^{2+} in pairs, and Co^{2+} in larger ionic clusters) changes, as well as the extent of ionic interactions among Co^{2+} ions, and the electronic properties of the solid in general. The concentration and the role of each specific configuration are now considered.

A homogeneous dispersion of Co^{2+} ions in the MgO matrix can be treated by statistical methods in order to find the probability (and hence the concentrations) that a given configuration of Co^{2+} ions exists. The method is essentially that adopted by Behringer for bulk configurations (*17*), but when the surface is considered the number of possibilities is greatly enlarged. Before entering into a description of the configurations, L, which have been worked out, and of the results obtained, it is appropriate to state the objectives of the present approach.

It was noted before that N_{ion} is not constant over the concentration range explored, and this means that not all ions (or, at least, not a constant fraction of the available ions) are active. On the other hand, if only a specific configuration L is active, the R values should be divided by the concentration of L ($=[L]$) to obtain the turnover number specific for a given configuration ($N_L = R/[L]$). One could then see which type of configuration L gives a reasonable constancy of N_L over the whole range of $[Co^{2+}]$.

The approach has limitations, since it assumes that a given configuration has a constant activity irrespective of its concentration, and it also disregards possible contributions of configurations related to, but not the same as, that considered. It should also be clear that the turnover numbers calculated for each configuration are lower limits since in reality only a fraction of the whole population of configurations could be working. For instance, only a few may effectively be bare, or a configuration, in order to be active, must also be close to some type of defect (such as a vacancy). If we assume, an as approximation, that the effective fraction of the active configuration is not too dependent on cobalt concentration, then the only quantity which depends on cobalt concentration will be the configuration concentration.

Concentration dependence of typical surface configurations. Turning to a description of the configurations, it may be noted that (i) different surface planes can be taken, and (ii) the definition of the configuration implies a definition of "isolation" of the ion(s) which depends on the type of interaction which is considered of importance. Point (i) can be covered by taking planes which show a marked variation in the cation/anion ratio, typically planes (100) and (111). The approach is admittedly schematic, but it will be shown that the concentration dependence of the various configurations is not very sensitive to the plane.

A more subtle, and very important point is point (ii). We can define that an ion A is isolated (*a*) if no neighbors A are present in the outer plane I, thus allowing A atoms to be neighbors if belonging to the plane underneath II (or III, if so required by the lattice geometry). Alternatively, we can say (*b*) that for an ion to be isolated it is necessary that no neighbors A are present either in the surface plane, or in the plane below. The first case (*a*) focuses attention on the availability of the neighboring ions as an (exposed) chemisorptive site, i.e., on the *geometry of the activated complex*. The second assumption (*b*) focusses attention on the *electronic interactions*, since these interactions take place also from underlying layers.

A further geometrical consideration is that the rock-salt structure of MgO allows two possibilities of defining a "neighbor": nearest neighbors along the [110] direction in the (100) plane, which corresponds to a direct Co^{2+}–Co^{2+} interaction, hereafter called *cc*, and the "anion-mediated" neighbors (such as along the [001] direction in the (100) plane), hereafter called *cac*.

The increase of N_{ion} with cobalt concentration suggests that nonisolated ions are required. Accordingly, an important configuration to be considered is a pair of Co^{2+} ions, or "dimer configuration." The

dimer configuration D has been calculated for dimers fully belonging to the outer plane I. Other dimers are those such that one atom A_1 belongs to I, and the other atom A_2 is underneath I. This dimer is physically less significant, because the site interacting with the gas would be A_1, the presence of A_2 making itself felt either by electronic interaction (thus becoming equivalent to the case of single ions not isolated from those in layer II) or by vacancies existing in I, which uncover sites A_2 in II. However, the latter case corresponds to a *surface* dimer belonging to a different plane.

We have examined various cases corresponding to definitions of isolation (*a*) and (*b*) above, i.e., planes (100) and (111); interactions of the type *cc*, *cac*, or both, and the probability functions have been worked out for single sites (whose concentration will be designated as [S], pairs or dimers [D], and all configurations but single [M].

The functional dependences of the concentration for the surface configurations S, D, and M are of the form:

$$[\mathrm{S}] = np(1 - p)^b, \tag{1}$$

$$[\mathrm{D}] = mnp^2(1 - p)^b, \tag{2}$$

$$[\mathrm{M}] = np - np(1 - p)^b, \tag{3}$$

where n is the total number of cations per unit area (Co + Mg atoms per square meter), m is the multiplicity factor, arising from different equivalent options in the choice of the position of the second ion A_2 in the dimer, b is an exponent which reflects the number of sites not occupied by A, and p is the mole fraction of A.

It would be too lengthy and not essential to give a complete list of the functional dependence for all configurations. We have focussed our attention on some which have a more direct physical meaning. Table 1 gives the values of m and b for a number of configurations specified by their symbols.

TABLE 1

Values of m and b for Some Typical Surface Configurations

Surface configuration	m	b
(a) Isolated ions on the (100) planes		
S (100) I (*cac*)	1	4
S (100) I (*cc*)	1	4
S (100) I, III (*cac*)	1	5
S (100) I (*cc, cac*)	1	8
S (100) I, II (*cc*)	1	8
S (100) I, II, III (*cc, cac*)	1	13
(b) Isolated ions on the (111) plane		
S (111) I (*cac*)	1	0
S (111) I, III (*cac*)	1	3
S (111) I (*cc*)	1	6
S (111) I (*cc, cac*)	1	6
S (111) I, III (*cc*)	1	9
S (111) I, III (*cc, cac*)	1	12
(c) *cac* dimers on the (100) plane		
Dcac (100) I (*cac*)	4	6
Dcac (100) I (*cc, cac*)	4	12
(d) *cc* dimers on the (100) plane		
Dcc (100) I (*cc*)	4	6
Dcc (100) I, II (*cc*)	4	12
(e) *cc* dimers on the (111) plane		
Dcc (111) I (*cc*)	6	8
Dcc (111) I, III (*cc*)	6	13

The designation of the concentration of the various configurations follows a key which includes: first, a letter indicating the type of configuration, viz., S, D, or M, and (for dimers) the type of dimer, *Dcc* or *Dcac*, considered; second, the Miller indices of the plane considered, (100) or (111); third a Roman numerical indicating the planes within which interactions are excluded: I (outer plane only), II and III underlying planes (from the surface to the interior); and fourth, the type of interaction excluded, viz., *cc*, *cac*, or both (*cc, cac*). Thus, the symbol "S(100)I *cac*" designates isolated ions present on the surface plane (100), which exclude interactions *cac* with other A atoms; the symbol *Dcc* (100) I (*cc, cac*) designates surface dimers of type *Dcc*, which exclude further interactions with A atoms in the plane I, either *cc* or *cac*; the symbol S (111) I, III (*cc, cac*) indicates isolated surface

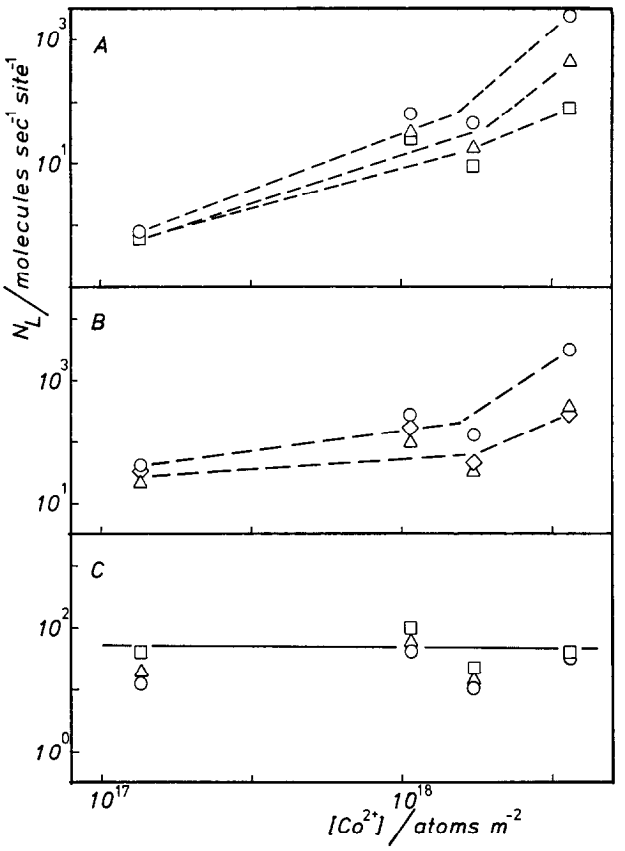

FIG. 4. A plot of N_L per molecules per second per site vs $[Co^{2+}]$ per atoms per square meter. Parts *A*, *B*, and *C* of the figure refer to the three cases L = S, D, and M, in that order. *A*: ○, S (100) I, II, III (*cc*, *cac*) ≃ S (111) I, III (*cc*, *cac*); △, S (100) I, II (*cc*) = S (100) I (*cc*, *cac*) ≃ S (111) I, III (*cc*); □, S (100) I (*cc*) = S (100) I (*cac*). *B*: ○, D*cac* (100) I (*cc*, *cac*) = D*cc* (100) I, II (*cc*) ≃ D*cc* (111) I, III (*cc*); △, D*cc* (111) I (*cc*) ≃ D*cac* (100) I, III (*cac*); ◇, D*cc* (100) I (*cc*) = D*cac* (100) I (*cac*). *C*: For M configurations the same symbols as for the corresponding S configurations are adopted.

ions, which exclude interaction with other A atoms both in plane I and III (plane II is only made by anions in the [111] direction) either *cc* or *cac*. Trimers or higher-order clusters have not been considered.

Turnover number per active configuration. From the Eqs. (1), (2) and (3), and with the help of Table 1, the numerical values of N_L for L = S, D, and M have been calculated from the H_2–D_2 experimental data. The results are shown in Fig. 4. The figure is divided into three sections, and plots N_L at 455 K as a function of $[Co^{2+}]$ (atoms per square meter) for the three cases L = S, L = D, and L = M. It can be seen that detailed analysis of the type of interaction (*a* or *b*, *cc*, or *cac*, or both) is much less important than whether or not a neighbor *tmi* is present, i.e., (S, D, M). In addition, the plane does not have a marked effect.

It is instructive to plot the ratio of the largest to the smallest N_L (which we shall term the "discrepancy factor") against some typical configurations (Fig. 5). One can see that the ratio decreases from a maximum of about 2.5×10^3 to about 1.1 as we pass from S to M.

Physical significance of the discrepancy

factor. The physical implications of the various configurations can now be considered. The requirement that an ion can be considered as isolated only if all interactions, *cc* and *cac*, are absent, either in the plane or between the two outer planes, is the most stringent one: S (100), I, II, III (*cc*, *cac*). This is the configuration which gives the largest discrepancy and shows that truly isolated ions cannot be active. The configuration S (100) I (*cc*, *cac*) fully isolates the ion in the external plane, but interactions with ions placed below are allowed. It is therefore conceivable that defects (vacancies, edges) and high index planes render the ion below more accessible, and the configuration is effectively "less isolated." It is not surprising then that the discrepancy factor decreases, although it is still large. Configurations which do not fully isolate the ion, such as S (100) I (*cc*) and S (100) I (*cac*), where interactions *cac* and *cc* are each allowed, give increasingly higher probabilities of finding a dimer. The discrepancy factor goes down to 84 (Surface configuration 3 in Fig. 5), a figure large enough to exclude these isolated configurations as effective ones.

The general situation for dimers is better. One can see, however, that D*cc* (100) I, II (*cc*) (Surface configuration 4 in Fig. 5), which still shows a large discrepancy factor, takes into account dimers which are fully isolated. The discrepancy factor is reduced if surface dimers are considered, such as D*cc* (100) I (*cc*) or D*cac* (100) I (*cac*), which allow further interactions (Surface configuration 6 in Fig. 5).

Finally, we can see what happens if isolated ions are excluded. The discrepancy factor is now only 2.6 (Surface configuration 7 in Fig. 5) if totally isolated ions are excluded, which is reduced to 1.1 (Surface configuration 9 in Fig. 5) if all configurations containing isolated ions are left out.

The reduction of the discrepancy factor

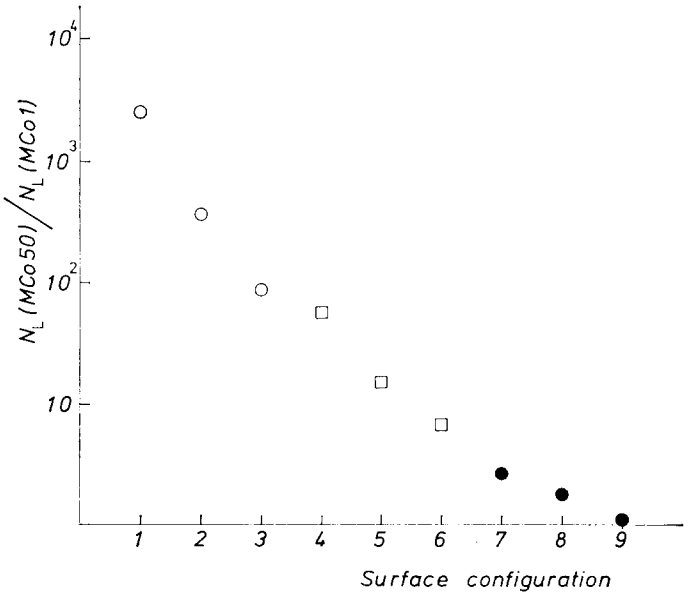

FIG. 5. Ratio of the largest to the smallest N_L obtained on the catalysts MCo 50 and MCo 1, respectively for S (○), D, (□), and M (●) configurations. 1: S (100) I, II, III (*cc*, *cac*); 2: S (100) I (*cc*, *cac*); 3: S (100) I (*cc*) and S (100) I (*cac*); 4: D*cc* (100) I, II (*cc*) and D*cac* (100) I (*cc*, *cac*); 5: D*cc* (111) I (*cc*); 6: D*cc* (100) I (*cc*) and D*cc* (100) I (*cac*); 7–9: M configurations, which correspond to S configurations in 1, 2 and 3, in that order.

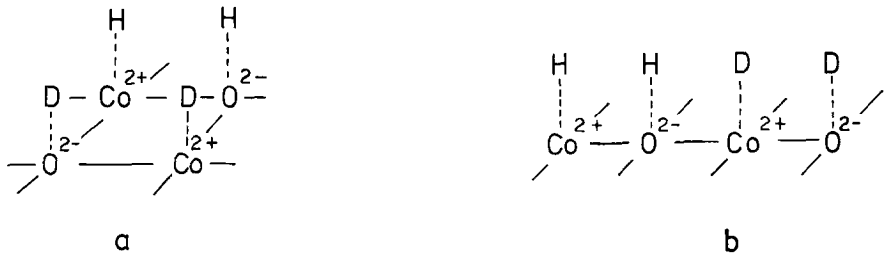

FIG. 6. Surface Co^{2+} dimers.

to this low level indicates that this approach is meaningful and shows that the active Co^{2+} ions must belong to a dimer or to a higher-order cluster. In orher words, one should not restrict attention to isolated dimers, and any pair, either isolated or belonging to a cluster, can be the active site.

2. *Nature of Active Centers and the H_2–D_2 Mechanism*

The requirement for the presence of a dimer or higher-order cluster in the center active for the H_2–D_2 equilibration in the HTR, focusses attention on (i) the problem of the mechanism and (ii) the nature of the active site to which the Co^{2+} dimer belongs.

At sufficiently high temperatures the hydrogen adsorption is thought to take place through the heterolytic dissociation of hydrogen molecules at cation–anion centers (*18*). The temperature at which dissociative adsorption prevails will depend on the acid–base properties of the cation–anion site, being favored by an increasing acid character of the cation and basic character of the anion.

Adsorption of H_2 (D_2) on diluted specimens yields surface species such as:

$$\begin{array}{llllll} H^- & H^+ & & & D^- & D^+ \\ | & | & & & | & | \\ Co^{2+}\text{–}O^{2-}\text{–}Mg^{2+}\text{–}O^{2-} & \cdots & & & Co^{2+}\text{–}O^{2-} & \end{array}$$

in which the cation–anion couples, thought to be active for adsorption, are well separated for each another. Therefore, for H_2–D_2 exchange to occur, migration along the surface of mono-atomic forms of hydrogen must take place. Evidence for this mechanism, which is now generally accepted for oxides in the HTR, was previously given by Conner and Kokes (*19*), in describing hydrogen migration across the surface to explain the H_2–D_2 activity of ZnO. The migration process is, however, expected to be very slow in the diluted CoO–MgO specimens in view of the chemical nature of the matrix, which favors the trapping of hydrogen at the strongly basic O^{2-} sites of MgO.

An active site consisting of a four-atom center can then be proposed, containing two Co^{2+} and two O^{2-} ions. The Co^{2+} ions can be arranged at the opposite vertices of a square, as in the *cc* configuration (Fig. 6a) or in a row with the anions, as in the *cac* configuration (Fig. 6b). The former case is equivalent to that discussed by Stone (*20*), and adsorption of one H_2 molecule side by side with a D_2 molecule gives rise to a complex which can desorb two HD molecules, thus restoring the bare site. The second configuration can absorb one H_2 molecule and one D_2 molecule on a line, and one HD molecule can be desorbed. Subsequent adsorption of an H_2 or D_2 molecule can desorb a second HD molecule, and the process can continue. Both modes have features in common: (i) They involve a dimer; (ii) they are not limited to isolated dimers (thus any M configuration could work); and (iii) they do not involve migration of H atoms.

The nature of the two anions of the active site should also play an important

role, as indicated by the higher activity of Cr^{3+} when dissolved in a solid solution of Al_2O_3 as compared to the activity of the same ion in MgO (*10*). An acid matrix is in fact expected to form weaker O^{2-}–H^+ bonds, thus favoring the HD desorption. The decrease of k_{abs} in the HTR, noted when distinguishing the behavior in the HTR from in the LTR, may well be due to the formation of hydrogen strongly bonded in the hydroxyl form (*9*). It should be stressed, however, that, in a given matrix, the presence of a wide distribution of O^{2-} sites has been shown by ESR (*21*). These differ in their base character and electron-donor properties, depending upon coordination. Therefore, also on MgO, the Co^{2+}–Co^{2+} dimer of the most active sites can be thought of as associated with O^{2-} sites of proper coordination, so as to render the adsorbed protons more weakly bonded.

In this respect, the active configurations depicted in Fig. 6 could be those involving oxygen ions in a special unsaturation state. Thus, only a fraction of all configurations M could be effective, or, more generally, a distribution of activity among all configurations M can be envisaged, favoring those involving oxygen ions in special configurations.

3. *The Role of Specific Surface Configurations for N_2O Decomposition and CO Oxidation*

N_2O decomposition. The marked decrease of N_{ion} with increasing cobalt content found for N_2O decomposition on CoO–MgO catalysts suggests that isolated ions are more active than those belonging to Co^{2+} clusters. It is true that differences in R values cannot be attributed simply to the variation of active site concentrations since they arise from the variation of both activation energy and pre-exponential factor, as shown by the E_a values which increase from 71.4 to 123.9 kJ mol^{-1} passing from MCo 0.05 to MCo 50 [Table 1 of Ref. (4)]. However, the approach of exploring the type of configuration L liable to give a constant N_L value can be used if the calculation of N_L is confined to the range MCo 0.1 to MCo 10 where the E_a values are roughly constant (84.0 to 94.5 kJ mol^{-1}). When this is done, the ratio of the largest to the smallest N_L, which is 10^2 for N_{ion}, becomes 25 if the isolated ion configuration S (100) I, II, III (*cc, cac*) is assumed. It is significant that the ratio increases if nonisolated ions are considered, and the ratio becomes very large for dimers: 1.5×10^3 for the D*cac* (100) I (*cc, cac*) and D*cc* (100) I, II (*cc*).

Thus, the large value of the discrepancy factor for any surface configuration, underlines that the dilution effect is not simply due to a requirement for a particular arrangement of atoms within the active site. This conclusion is supported by a comparison with the Co^{2+} concentration dependence in other matrices. Only the MgO matrix shows such a marked decrease of N_{ion} with increasing cobalt content (*22*). This fact suggests a possible role of the MgO matrix. The role of the matrix, which influences not only the symmetry of the site but also the modes of oxygen migration and release, has been discussed in several papers from this laboratory (*4, 23–26*) as well as in review articles (*1, 2*). It is useful to recall briefly that the proposed mechanism of N_2O decomposition on Co^{2+}-containing systems can be summarized by the following equations:

$$N_2O + Co^{2+} \xrightarrow[(4a)]{} N_2O^- \cdots Co^{3+} \xrightarrow[(4b)]{} N_{2(g)} + Co^{3+} \cdots O^- \quad (4)$$

$$Co^{3+} \cdots O^- \xrightarrow[(5a)]{+Co^{3+} \cdots O^-} O_{2(g)} + 2Co^{2+} \quad (5)$$

$$\xrightarrow[(5b)]{+Co^{2+}} O^{2-} + 2Co^{3+}$$

$$\xrightarrow[(5c)]{+O^{2-}} Co^{2+} \cdots O_2^{2-}$$

$$O_2^{2-} + O^{2-} \xrightarrow[(6a)]{} O^{2-} + O_2^{2-} \quad (6)$$

$$O_2^{2-} + O_2^{2-} \xrightarrow[(6b)]{} O_{2(g)} + 2O^{2-}$$

According to this scheme, stesps (4a) and (4b) are independent of cobalt content except for electronic factors arising from ionic interactions. Step (5a) would be favored by an increase of $[Co^{2+}]$, and therefore, in view of the decrease of N_L with $[Co^{2+}]$, cannot play a significant contribution to oxygen desorption. The desorption can be accomplished through the participation of surface O^{2-} ions: (5c), (6a), and (6b) ("peroxide mode") (*1*). Adducts of oxygen species to Co^{3+} have been recently investigated by ESR methods in our laboratory (*27*), and evidence was found of a high lability of $Co^{3+}\cdots O_2^-$ and of $Co^{3+}\cdots O^-$ surface complexes, which are thought to release oxygen species to other O^{2-} sites of the MgO matrix. The "oxygen spillover" originated by activation at Co^{2+} sites and subsequently carried out by the matrix can be described by the steps (4), (5c), and (6). It is then understandable why the MgO matrix, which is particularly able to form peroxide species, plays a unique role. The decrease of N_L in CoO–MgO specimens would then reflect the ease of occurrence of the peroxide mode in dilute specimens, in accordance with one of the cases, mentioned in the Introduction, which can contribute to the dilution effect.

CO oxidation. In view of the constancy of the N_{ion} value over the whole range of cobalt concentrations it can be argued that each individual Co^{2+} ion is active, irrespective of whether it belongs to a cluster or not. The constancy within each matrix has been confirmed on other Co^{2+}-containing systems investigated in our laboratory (MgO–ZnO; ZnO; $MgAl_2O_4$) (*6*). The CO oxidation thus appears to be a "structure-insensitive" reaction. A similar intermediate complex can then be envisaged for all systems, but the formation of the complex points to the participation of neighboring anions. A possible intermediate is:

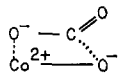

where a carbonate surface complex is formed. Similar surface complexes have been observed by infrared spectroscopy on pure cobalt oxides (*28–29*). The constancy of N_{ion} and of E_a, the possible influence of the anion character, and the requirement of oxygen presence are accounted for by the scheme (details will be discussed elsewhere).

CONCLUDING REMARKS

The pattern of activity for the H_2–D_2 equilibration with varying Co^{2+} concentration in the MgO matrix has allowed a mechanism to be formulated which requires the presence of at least two neighboring Co^{2+} ions. The reaction is therefore configuration dependent. Comparison with other simple reactions shows that CO oxidation is not configuration dependent, and that for the N_2O decomposition the concentration dependence of the turnover number must arise not from a configuration requirement, but from oxygen desorption modes, in addition to possible electronic effects.

REFERENCES

1. Cimino, A., *Chim. Ind.* **56**, 27 (1974).
2. Stone, F. S., *J. Solid State Chem.* **12**, 271 (1975).
3. Boreskov, G. K., *in* "Proceedings. 6th International Congress on Catalysis," 1976, London (G. C. Bond, P. B. Wells, and F. C. Tompkins, Eds.), p. 204. Chemical Society, London, 1977.
4. Cimino, A., and Pepe, F., *J. Catal.* **25**, 362 (1972).
5. Boudart, M., *in* "Advances in Catalysis" (D. D. Eley, H. Pines, and P. B. Weisz, Eds.), Vol. 20, p. 153. Academic Press, New York, 1969.
6. Cimino, A., Indovina, V., and Pepe, F., Gazzetta Chim. Ital., to be published.
7. Cimino, A., Lo Jacono, M., Porta, P., and Valigi, M., *Z. Phys. Chem. N.F.* **70**, 166 (1970).

8. Cimino, A., De Angelis, B., Minelli, G., Persini, T., and Scarpino, P., to be published.

9. Indovina, V., Cimino, A., and Valigi, M., *in* "Proceedings. 6th International Congress on Catalysis," 1976, London (G. C. Bond, P. B. Wells, and F. C. Tompkins, Eds.), p. 213. Chemical Society, London, 1977.

10. Indovina, V., Cimino, A., and Inversi, M., *J. Phys. Chem.* **82**, 285 (1978).

11. Stone, F. S., and Vickerman, J. C., *Proc. Roy. Soc. Ser. A* **354**, 331 (1977).

12. Vickerman, J. C., *J. Catal.* **44**, 404 (1976).

13. Kokes, R. J., *Accounts Chem. Res.* **6**, 226 (1973).

14. Fukushima, T., and Ozaki, A., *J. Catal.* **41**, 82 (1976).

15. Burwell, R. L., and Stec, K. S., *J. Colloid Interface Sci.* **58**, 54 (1977).

16. (a) Thomas, J. M., and Thomas, W. J., "Introduction to the Principles of Heterogeneous Catalysis," p. 301. Academic Press, New York, 1967; (b) Boudart, M., *in* "Kinetics of Chemical Processes," p. 35 and 82. Prentice-Hall, Englewood Cliffs, N. J., 1968.

17. Behringer, R. E., *J. Chem. Phys.* **29**, 537 (1958).

18. Burwell, R. L., Haller, G. L., Taylor, K. C., and Read, J. F., *in* "Advances in Catalysis" (D. D. Eley, H. Pines, and P. B. Weisz, Eds.), Vol. 20, p. 1. Academic Press, New York, 1969.

19. Conner, W. C., and Kokes, R. J., *J. Catal.* **36**, 199 (1975).

20. Stone, F. S., *Chimia* **23**, 490 (1969).

21. (a) Cordischi, D., and Indovina, V., *J. Chem. Soc. Faraday Trans. I* **72**, 2341 (1976); (b) Cordishchi, D., Indovina, V., and Occhiuzzi, M., *J. Chem. Soc. Faraday Trans. I* **74**, 456 (1978).

22. Cimino, A., Indovina, V., Pepe, F., Schiavello, M., and Angeletti, C., to be published.

23. Cimino, A., and Indovina, V., *J. Catal.* **17**, 54 (1970).

24. Schiavello, M., Cimino, A., and Criado, J. M., *Gazz. Chim. Ital.* **101**, 47 (1971).

25. Cimino, A., Pepe, F., and Schiavello, M., *in* "Proceedings. 5th International Congress on Catalysis," Florida 1972 (J. W. Hightower, Ed.), p. 125. North-Holland, Amsterdam, 1973.

26. Pepe, F., Schiavello, M., and Ferraris, G., *Z. Phys. Chem. N.F.* **96**, 297 (1975).

27. Cordischi, D., Indovina, V., Occhiuzzi, M., and Arieti, A., *J. Chem. Soc. Faraday Trans. I* **75**, 533 (1979).

28. Goodsel, A. J., *J. Catal.* **30**, 175 (1973).

29. Hertl, W., *J. Catal.* **31**, 231 (1973).